UC Irvine
UC Irvine Previously Published Works

Title

Neutrophil IL-1β Processing Induced by Pneumolysin Is Mediated by the NLRP3/ASC Inflammasome and Caspase-1 Activation and Is Dependent on K+ Efflux

Permalink

Journal

ISSN

Authors

Karmakar, Mausita
Katsnelson, Michael
Malak, Hesham A
et al.

Publication Date

DOI

Peer reviewed

Neutrophil IL-1β processing induced by pneumolysin is mediated by the NLRP3/ASC inflammasome and caspase-1 activation, and is dependent on K+ efflux

Mausita Karmakar[*], **Michael Katsnelson**[†], **Hesham A. Malak**[§], **Neil G. Greene**[‡], **Scott J. Howell**[*], **Amy G. Hise**[¶], **Andrew Camilli**[‡], **Aras Kadioglu**[§], **George R. Dubyak**[†], and **Eric Pearlman**[*,‖]

[*]Department of Ophthalmology and Visual Sciences, Department of Clinical Infection, Microbiology and Immunology, Institute of Infection and Global Health, University of Liverpool, Liverpool, UK

[†]Department of Physiology and Biophysics, Tufts University School of Medicine, Boston, MA

[‡]Howard Hughes Medical Institute and Department of Molecular Biology and Microbiology and Graduate Program in Molecular Microbiology, Sackler School of Graduate Biomedical Sciences, Tufts University School of Medicine, Boston, MA

[§¶]Department of Medicine, Louis Stokes Cleveland Veterans Affairs Medical Center, Cleveland, OH

Abstract

Although neutrophils are the most abundant cells in acute infection and inflammation, relatively little attention has been paid to their role in inflammasome formation and IL-1β processing. In the current study, we investigated the mechanism by which neutrophils process IL-1β in response to *Streptococcus pneumoniae*. Using a murine model of *S. pneumoniae* corneal infection, we demonstrated a requirement for IL-1β in bacterial clearance, and showed that NLRP3, ASC and caspase-1 are essential for IL-1β production and bacterial killing in the cornea. Neutrophils in infected corneas had multiple specks with enzymatically active caspase-1 (FLICA-660+), and bone marrow neutrophils stimulated with heat killed *S. pneumoniae* (signal 1) and pneumolysin (signal 2) exhibited multiple specks after staining with FLICA-660, NLRP3 or ASC. High molecular weight ASC complexes were also detected, consistent with oligomer formation. Pneumolysin induced K^+ efflux in neutrophils, and blocking K^+ efflux inhibited caspase-1 activation and IL-1β processing; however, neutrophils did not undergo pyroptosis, indicating that K^+ efflux and IL-1β processing is not a consequence of cell death. There was also no role for lysosomal destabilization or neutrophil elastase in pneumolysin mediated IL-1β processing in neutrophils. Together, these findings demonstrate an essential role for neutrophil derived IL-1β in *S. pneumoniae* infection, and elucidate the role of the NLRP3 inflammasome in neutrophil cleavage and secretion of mature IL-1β. Given the ubiquitous presence of neutrophils in acute bacterial and fungal infections, these findings will have implications for other microbial diseases.

[‖]To whom correspondence should be addressed: Eric Pearlman, Department of Ophthalmology and Visual Sciences, Case Western Reserve University, 10900 Euclid Ave, Cleveland OH 44095. eric.pearlman@case.edu; Tel: 216 368 1856. Fax: 2163683171.

INTRODUCTION

IL-1β plays an important role in multiple infectious and acute and chronic inflammatory diseases, including diabetes and ischemic injury, and is a target for anti-inflammatory therapies (1, 2). Following activation of TLRs or other pathogen recognition molecules, IL-1β is translated as an inactive 34kD pro-form, which is subsequently cleaved to the active, 17kD form that can be secreted (3, 4). Although we, and others demonstrated a role for neutrophil proteases in cleavage (5–7), caspase-1 is the main enzyme that cleaves the IL-1β pro-form in macrophages and dendritic cells. Caspase-1 is also produced as an inactive pro-form that auto-catalyzes its cleavage to the enzymatically active caspase-1, which occurs following oligomerization of inflammasome components, including the Nod-like receptor protein 3 (NLRP3) together with the adaptor molecule apoptosis-associated speck like protein containing a caspase recruitment domain (ASC) (3, 8).

In the current study, we demonstrate that neutrophils are the predominant source of IL-1β in a murine model of acute *Streptococcus pneumoniae* corneal infection, and that IL-1β cleavage is dependent on the NLRP3/ASC inflammasome, and active caspase-1, which are detected as large, intracellular specks in neutrophils both *in vitro* and during infection. Further, using highly purified human neutrophils, we show that secretion of mature IL-1β is induced by bacterial pneumolysin, and that the mechanism requires a rapid efflux of K^+ ions that precedes NLRP3 inflammasome activation and IL-1β cleavage without undergoing pyroptosis. Together, these findings elucidate a critical role for the NLRP3/ASC inflammasome and caspase 1 in IL-1β processing and secretion by neutrophils.

MATERIALS AND METHODS

Source of mice

C57BL/6 mice (6–10 weeks old) were from The Jackson Laboratory (Bar Harbor, ME), IL-1β$^{-/-}$ mice were obtained from Dr. Iwakura (University of Tokyo, Japan). Caspase-1/11$^{-/-}$ mice were generated by Richard Flavell (Yale University, CT) as Caspase-1$^{-/-}$ mice (9), and subsequently found to be also deficient in caspase 11 (8, 10). NLRP3$^{-/-}$ and ASC$^{-/-}$ mice were generated by Millennium Pharmaceuticals (Cambridge, MA). The NLRP3$^{-/-}$ mice were generated by homologous recombination in embryonic stem cells by replacing exons I and II of the cryopyrin gene (encoding the amino-terminal Pyrin domain) with an IRES-β-gal-neomycin resistance cassette therefore they are functional rather than complete knockout mice (11). Neutrophil elastase (NE)$^{-/-}$ mice were purchased from The Jackson Laboratory. All knockout mice were on C57BL/6 background. Animals were housed in pathogen free conditions in microisolator cages and were treated according to institutional guidelines after approval by the Case Western Reserve University IACUC.

Bacterial Strains and growth conditions

Wild type encapsulated *Streptococcus pneumoniae* TIGR4 (serotype IV) was used in this study. To generate *ply* deletion mutant, the Ply coding region of TIGR4 was replaced with an antibiotic resistance cassette encoding chloramphenicol acetyltransferase (cat) via transformation of competent cells with a linear splicing by overlap extension (SOE) PCR

product. Approximately 1 kb of flanking sequence on either side of ply was amplified from TIGR4 genomic DNA using primer sets SP_1923 F1/SP_1923 R1 and SP_1923 F2/ SP_1923 R2 (Supplemental Table S1) for upstream and downstream sequences, respectively. The cat cassette was PCR amplified from pEVP3 using primer set Fcat/Rcat and all three products were spliced together by SOE using primers SP_1923 F1 and SP_1923 R2. Competent cells of TIGR4 were transformed with the resulting amplicon and chloramphenicol-resistant colonies were selected on Fluka Blood Agar Base No. 2 (Sigma Aldrich) supplemented with 5% defibrinated whole sheep blood containing chloramphenicol (4μg/ml). PCR and DNA sequencing were carried out to confirm replacement of ply with the cat cassette. Both WT and ply strains were routinely grown in Todd-Hewitt Broth (Neogen) supplemented with 0.5% yeast extract in 37°C and 5% CO_2 incubator. Bacteria were grown to mid exponential phase such that there is 10^8CFU/ml and diluted in sterile PBS to desired concentrations for corneal infection or *in vitro* stimulation. To generate heat killed bacteria (hkSP), TIGR4 was diluted in sterile PBS and heated at 95°C for 5mins. Viability was confirmed by plating bacteria in trypticase soy agar plate containing 5% defibrinated sheep blood (BD).

Murine model of Streptococcus pneumoniae corneal infection

Mice were anesthetized with 1.2% 2,2,2 tribromoethanol and corneal epithelium of the mice was abraded using a 26-gauge needle through which a 2μl injection containing ~10^5 TIGR4 in sterile PBS was released into the corneal stroma using a 33-gauge Hamilton syringe and mice were allowed to recover from anesthesia. Infected mice were anesthetized after 24hrs and positioned in a three point stereotactic mouse restrainer to monitor corneal opacification using a stereomicroscope and Spot RT Slider KE camera (Diagnostics Instruments). Images were uploaded into Metamorph Image analysis software (Molecular Devices Corp) and percent and total opacity was quantified as described (6, 12). For depletion of neutrophils, mice were injected with 250μg of NIMP-R14 antibody or IgG by intraperitoneal injection 24hrs prior to infection with ~10^5 TIGR4.

Quantification of Streptococcal colony forming units (CFU)

For assessment of bacterial viability, infected mice were sacrificed by CO_2 asphyxiation and whole eyes were isolated and homogenized in 1ml sterile PBS in Mixer Mill MM300 (Retsch) at 33Hz for 3mins. Serial log dilutions of the bacteria were plated on blood agar plates, incubated in CO_2 incubator at 37°C for 18h and colony numbers were counted manually.

Source of reagents

Recombinant pneumolysin (Ply) was expressed in *E. coli* and purified as described (13, 14). Unless otherwise stated the specific hemolytic activity of Ply was 100,000 HU/mg. The toxin was passed three times through an EndoTrap endotoxin removal column (Profos AG, Germany) after which LPS was undetectable using the PyroGene Recombinant Factor C assay (Lonza; detection limit 0.01 EU/ml). NFκB inhibitor JSH23 (Sigma Aldrich) and pJNK/AP-1 inhibitor - SP600125 (Tocris Bioscience) were dissolved in DMSO and used at assay dependent concentrations. Caspase-1 inhibitor YVAD (Bachem) and pan caspase

inhibitor ZVAD (ApexBio) were dissolved in DMSO and used at indicated concentration. Bafilomycin A (LC laboratories), CA-074-Me (EMD Chemicals) and ZFA (Bachem) was dissolved according to manufacturer's protocol. Nigericin (Calbiochem) was used at 10μM concentration. High potassium medium for neutrophils had the following composition: 130mM KCl, 1.5mM CaCl2, 1mM MgCl2, 25mM HEPES, 5mM glucose and 0.1% BSA at pH 7.4. For low potassium medium, we add 5mM KCl keeping other components the same.

Flow Cytometry of corneas and Image Stream analysis

Corneas from infected mice were excised using a surgical micro-scissor and incubated in type I collagenase (Sigma) at 82U/cornea for 2h at 37°C. The cell suspension was then passed through 30μm filter to remove any undigested tissue. Fc receptors were blocked for 20 min at RT with anti-mouse CD16/32 antibody (eBiosciences) followed by incubation with Alexa488-NIMP-R14 (in-house) and PE-F4/80 (eBiosciences) antibodies to detect neutrophils and macrophages, respectively. After staining, cells were washed in 2mL of FACS Buffer (1% FBS in PBS) and fixed in 0.5% PFA for analysis by flow cytometry using Accuri C6 Flow cytometer (Becton Dickinson).

For intracellular cytokine staining, corneal cells were incubated at 4°C overnight with 1X Protein Transport Inhibitor Cocktail (eBiosciences), fixed in 4% paraformaldehyde and permeabilized in 1x Perm Buffer (eBiosciences) for 10mins. Cells were then stained with APC-pro IL-1β antibody (eBiosciences), washed in FACS buffer and fixed in 0.5% PFA for analysis by flow cytometry or Multispectral Imaging Flow Cytometry (Image stream-100, Amnis).

AMNIS ImageStreamX and IDEAS analysis

Purified bone marrow neutrophils were primed for 3h with hkSP (signal1) and then stimulated with Ply (200ng/ml). Unstimulated neutrophils were used as control. Following stimulation, the cells were stained with either FAM-YVAD-FMK (Immunochemistry) according to the manufacturer's protocol or with ASC monoclonal Ab (clone 2EI-7, Millipore) followed by anti-mouse e488 secondary antibody. Acquisition was performed using ImageStreamX Imaging Flow Cytometer (Amnis Corporation, Seattle, WA) equipped with INSPIRE software as described (15). Briefly, a 60X magnification was used to acquire images of all samples. A minimum of 10,000 cells were analyzed for each treated sample. FAM-YVAD-FMK stained cells (for caspase-1) and ASC stained cells were excited with a 100 mW of 488 nm argon laser and were collected on channel two (505–560 nm). Intensity adjusted brightfield images were collected on channel one. Data analysis was performed using the IDEAS software (Amnis Corporation). Data were compensated using a compensation matrix generated using singly stained samples. The compensated data was first gated to eliminate cells that were not in the field of focus; second, the focused cells were gated to eliminate clumped cells and debris. The IDEAS software contains wizards to measure features, such as 'count spots' associated with the cells. For the spot counting wizard, subpopulations of cells with no spots, low and high numbers of spots were manually identified as truth sets, and the software used these data sets to determine the number of spots per cell.

Western blot analysis

Corneas were excised from the eyes using a microscissor. Any associated iris was removed and clean corneas were homogenized in 1x cell lysis buffer (Cell Signaling Technology) supplemented with protease inhibitor cocktail. For *in vitro* experiment, 4×10^6 cells were lysed in cell lysis buffer after appropriate stimulation. 20–30μg of protein were fractionated in 12% SDS-PAGE, transferred into nitrocellulose membrane and incubated with primary antibodies – mouse IL-1β (R&D Systems), mouse NLRP3 and ASC (Adipogen), human NLRP3 (Sigma Aldrich) and ASC (Adipogen), mouse Caspase-1p10 (Santa Cruz), mouse pJNK (T183/Y185) and total JNK (Cell Signaling Technology) and β actin (Sigma Aldrich). Reactivity was determined using HRP-conjugated secondary antibodies (Santa Cruz) and developed with Supersignal West Femto Maximum Sensitivity Substrate (Pierce).

Isolation of human and mouse bone marrow neutrophils

Human neutrophils were isolated from the peripheral blood of healthy volunteers following informed consent as approved by the Institutional Review Board of University Hospitals of Cleveland. Heparinized blood was incubated with 3% dextran in PBS (Sigma Aldrich) for 20mins at RT. The top clear layer containing leukocytes was transferred to a fresh tube and the cells were underlaid with 10ml of Ficoll Paque Plus (GE Healthcare), and centrifuged at 300xg for 20min. The overlying plasma and PBMC layer was aspirated and the neutrophil/RBC pellets were suspended in 1x RBC lysis buffer (ebiosciences). Following this, cells were washed in sterile PBS and resuspended in RPMI+L-glutamine media (Hyclone) supplemented with 2% FBS (Mediatech). Cell purity was determined for each experiment by Wright-Giemsa (Sigma Aldrich) and routinely yielded >97% pure neutrophils.

For mouse bone marrow neutrophils, total bone marrow cells were collected from tibias and femurs. Neutrophils were isolated from the total bone marrow cells by negative selection using EasySep™ Mouse Neutrophil Enrichment Kit (Stem Cell). After magnetic separation, cells were washed with PBS and resuspended in RPMI+L-glutamine with 1% FBS. This procedure routinely yielded >94% pure neutrophils as quantified by Wright-Giemsa stain.

Caspase-1 activation assay

Active caspase-1 was quantified by using FLICA-660 (660-YVAD-FMK) far red detection kit (Immunochemistry Technologies) according to manufacturer's guidelines. Stained cells were either quantified by flow cytometry (using unstained cells to set the gate) or were visualized by confocal microscopy for active caspase-1 oligomerization.

Immunofluorescence staining

Stimulated human and mouse neutrophils were fixed with 4% PFA (Fisher) at RT for 15 min and permeabilized with 0.1% Triton-X 100 for 10 mins. Cells were then blocked in 10% goat or rabbit serum (Vector Laboratories) in PBS for 1h at 22°C, followed by staining with a monoclonal antibody to NLRP3 (clone EPR4777, Abcam) or ASC (Millipore) for 1h at 37°C. Cells were then washed 3X in PBS and counter stained with Texas red rabbit anti-goat

IgG (Vector Laboratories) or Alexa488 goat-anti mouse IgG (Invitrogen) for 40 min at RT. The cells were washed 3x in PBS and stained with DAPI.

Confocal Microscopy

Images were collected using UltraVIEW VoX spinning disk confocal system (Perkin Elmer) mounted on a Leica DMI6000B microscope equipped with a HCX PL APO 100 x/1.4 oil immersion objectives using a 0.2μm step size. Images were then imported into Metamorph Image Analysis Software (Molecular Devices Corp) where maximum projections were generated from the original stacks and visualized following 2D deconvolution.

ASC oligomerizarion assay

Stimulated murine neutrophils were lysed in RIPA lysis buffer (0.5% Na-deoxycholate, 0.1% SDS, and 1% NP-40) and centrifuged at 4000g for 10min. Lysate was transferred to a fresh tube, pellets were washed twice in 1x PBS and then cross-linked using DSS (final concentration is 2mM) for 30 min at room temperature. The cross-linked pellet was centrifuged at 4000g for 10 min. resuspended in Laemmli buffer and fractionated in 12% SDS-PAGE. Western blot analysis was performed using anti-ASC antibody.

Atomic Absorbance Spectroscopy

After stimulation of mouse or human neutrophils, the extracellular medium was aspirated and the cells were rapidly washed in potassium-free isotonic buffer (135mM sodium gluconate, 1.5mM $CaCl_2$, 1mM $MgCl_2$, and 25mM HEPES). The washed cell pellets were then extracted into 1ml of 10% HNO_3. K^+ content in the nitric acid extracts was quantified by atomic absorbance spectrometry (Agilent 55B AA) as described previously (16). Triplicate samples were run for all test conditions in each experiment.

Detection of cytokines by ELISA

Half well cytokine assays were performed using Duoset ELISA assay kit for IL-1β and CXCL8/IL-8 according to manufacturer's protocol (R and D Systems).

LDH release assay

After stimulation of neutrophils, supernatant was collected and LDH release was quantified using CytoTox 96® Non-Radioactive Cytotoxicity Assay (Promega) according to the manufacturer's instructions. Percentage cytotoxity was calculated based on LDH release in total cell lysate.

Statistical Analysis

Student t test or ANOVA with Tukey post hoc analysis (Prism, Graphpad Software) were used as indicated in the figure legends. A P value equal or less than 0.05 was considered significant.

RESULTS

NLRP3, ASC, Caspase-1 and IL-1β are required for protection against S. pneumoniae corneal infection

The normal avascular mammalian cornea has resident macrophages and dendritic cells, whereas neutrophils are only detected following an infectious or inflammatory event when they are recruited from peripheral, limbal vessels together with infiltrating macrophages and dendritic cells (17, 18). To examine the role of IL-1β on bacterial growth and corneal disease severity following corneal infection, *S. pneumoniae* strain 1 x 10^5 bacteria of strain TIGR4 were injected into the corneal stroma of C57BL/6 or IL-1β$^{-/-}$ mice. After 24h, the total number of bacteria was assessed by colony forming units (CFU), and the number of infiltrating neutrophils and macrophages were quantified by flow cytometry using the NIMP-R14 antibody (recognizes Ly6G receptor) which we have shown reacts specifically with neutrophil (19), and the F4/80 antibody that primarily detects macrophages.

Quantification of infiltrating cells in the cornea showed significantly less neutrophils in infected IL-1β$^{-/-}$ compared with C57BL/6 corneas, whereas there was no significant difference in the number of infiltrating macrophages (Figure 1A). Conversely, we found significantly higher CFU in IL-1β$^{-/-}$ corneas compared with C57BL/6 corneas (Figure 1B). Representative bright field images of *S. pneumoniae* infected corneas show severe corneal opacity in C57BL/6 compared with IL-1β$^{-/-}$ corneas (Figure 1C), and quantification of corneal opacity revealed significantly higher corneal disease in C57BL/6 compared with IL-1β$^{-/-}$ mice (Figure 1D, E). IL-1β$^{-/-}$ corneas perforate after 48h due to unrestricted bacterial growth (data not shown). Hematoxylin and eosin staining of corneal sections from infected eyes showed enhanced cellular infiltration in the corneal stroma of infected C57BL/6 compared with IL-1β$^{-/-}$ mice, which was comprised mostly of NIMP-R14$^+$ neutrophils (Supplemental Figure S2).

Although we found no role for caspase-1 in *Pseudomonas aeruginosa* keratitis (6), we examined if this protease was required for clearance of *S. pneumoniae*. Corneas of Caspase-1/11$^{-/-}$ mice were therefore infected, and cellular infiltration, CFU and corneal opacity were measured as before. As shown in Figures 1F–J, Caspase-1/11$^{-/-}$ mice had the same phenotype as IL-1β$^{-/-}$ mice, with significantly less neutrophil infiltration (Figure 1F), impaired bacterial clearance (Figure 1G), and less corneal opacification (Figure 1H–J). Similar results were found for NLRP3$^{-/-}$ and ASC$^{-/-}$ mice compared with C57BL/6 mice (Figure 1K–O).

Taken together, these data clearly implicate a role for IL-1β and the NLRP3/ASC inflammasome in regulating neutrophil infiltration and bacterial growth in *S. pneumoniae* corneal infection.

NLRP3 and ASC are required for caspase-1 activation and IL-1β processing by neutrophils during S. pneumoniae corneal infection

To assess whether the NLRP3/ASC inflammasome is required for IL-1β processing *in vivo*, corneas of C57BL/6, NLRP3$^{-/-}$ and ASC$^{-/-}$ mice were infected with *S. pneumoniae* as described above, and after 24h, corneas were homogenized and processed for western blot

analysis. Figure 2A shows the p10 caspase-1 subunit and the processed p17 IL-1β bands in infected C57BL/6 corneas, but not in infected NLRP3$^{-/-}$ or ASC$^{-/-}$ corneas. Further, ASC was present in the PBS treated mice, whereas NLRP3 was detected only after *S. pneumoniae* infection.

To identify the cells producing intracellular pro-IL-1β, corneas of C57BL/6 mice were infected with *S. pneumoniae* as before, and after 24h, corneas were digested with collagenase, and cells were stained with NIMP-R14, F4/80 and intracellular IL-1β and examined by flow cytometry. We found a distinct population of neutrophils in infected corneas expressing intracellular pro-IL-1β, comprising more than 20% of the total corneal cells (Figure 2B). Further, 85% of total pro IL-1β producing cells in the cornea were NIMP-R14$^+$ neutrophils compared with F4/80$^+$ macrophages, which accounted for less than 15% of the total IL-1β positive cells (Figure 2B).

To determine if neutrophils are producing active caspase-1, *S. pneumoniae* infected C57BL/6 corneas were digested with collagenase, and total corneal cells were stained with NIMP-R14 and FLICA660-YVAD, a fluorescent peptide that binds to active caspase-1 and which has been used to detect active caspase-1 in macrophages (20, 21). We found that > 30% of total cells in the cornea were FLICA-660 YVAD positive neutrophils, and >75% caspase-1 positive cells in the cornea were NIMP-R14$^+$ neutrophils (Figure 2C). Active caspase-1 in neutrophils was also detected as speck-like aggregates as shown by multispectral imaging flow cytometry (Figure 2D).

To examine the role of neutrophils in IL-1β processing and NLRP3 expression, neutrophils were depleted in C57BL/6 mice by intraperitoneal injection of NIMP-R14 antibody 24hr before infection with *S. pneumoniae*. Systemic neutrophil depletion was confirmed by flow cytometry (Supplemental Figure S3), and corneas from *S. pneumoniae* infected mice were examined for NLRP3 and IL-1β production. As shown in Figure 2E, there was decreased expression of NLRP3 and pro-IL-1β in neutrophil depleted mice, and no mature IL-1β in was detected. In addition, there was decreased corneal opacity (Figure 2F) and significantly increased CFU in neutrophil depleted mice (Figure 2G). These findings support the concept that neutrophils are essential for production of mature IL-1β, and for bacterial killing. Although we cannot eliminate the possibility of an indirect role on macrophage infiltration, combined data in this figure indicate that neutrophils are the major source of IL-1β in *S. pneumoniae* corneal infection.

NLRP3/ASC expression and oligomerization in murine bone marrow neutrophils

To examine the expression of NLRP3 and ASC, bone marrow neutrophils from C57BL/6 and NLRP3$^{-/-}$ mice were incubated for 3h with heat killed *S. pneumoniae* (**hkSP**) (Signal 1), and proteins were detected by western blot. NLRP3 expression was low in unstimulated neutrophils, but was induced over time after stimulation with hkSP as signal 1 (Figure 3A). In contrast, ASC was constitutively expressed in unstimulated C57BL/6 and NLRP3$^{-/-}$ neutrophils (Figure 3A).

As TLR2 is elevated in corneas of individuals with *S. pneumoniae* corneal ulcers, and TLR2 modulates the severity of murine *S. pneumoniae* corneal infection (22, 23), we examined the

role of TLR2 in NLRP3 and ASC expression. Bone marrow neutrophils from C57BL/6 and TLR2$^{-/-}$ mice were stimulated 3h with hkSP, and NLRP3 and ASC expression were detected by western blot analysis. Figure 3B shows decreased NLRP3 expression in TLR2$^{-/-}$ compared with C57BL/6 neutrophils, whereas expression of ASC remained unchanged. To examine other mediators of TLR2 signaling on NLRP3 expression, C57BL/6 neutrophils were incubated with the NFκB inhibitor JSH-23 or the JNK inhibitor SP600125. We found that NLRP3 expression was completely inhibited in the presence of JSH-23 and partially inhibited by SP600125 (Figure 3C, D), although there was no effect of either inhibitor on ASC expression.

Together, these data indicate that *S. pneumoniae* induces NLRP3 expression by TLR2 activation through the NFκB and to some extent the MAPK/AP-1 pathway, whereas ASC expression in neutrophils is constitutive.

The active NLRP3 inflammasome forms large, multimeric complexes with ASC in macrophages and dendritic cells (3, 24); however, this has not been clearly shown for neutrophils. To investigate NLRP3 and ASC oligomerization in neutrophils, bone marrow neutrophils from C57BL/6 mice were incubated 3h with hkSP (Signal 1), followed by 2h stimulation with live WT TIGR4, recombinant hemolytic pneumolysin (Ply) or with the inactive Ply toxoid (PdB) as Signal 2, and intracellular NLRP3 was detected by confocal microscopy using the same monoclonal antibody to NLRP3 (clone EPR4777, Abcam) used by others (25, 26). NLRP3 expression was very low in unstimulated neutrophils; however, following incubation with hkSP, there was enhanced NLRP3 expression in the cytosol (Figure 3E). This is also consistent with our observation in Figure 3A that priming with hkSP induces NLRP3 expression in murine and human neutrophils. However, after further incubation with live TIGR4 or active pneumolysin (Ply), NLRP3 was detected as speck-like aggregates in neutrophils. Further, specks were not detected in neutrophils incubated with non-hemolytic PdB. This diffuse staining with signal 1 and the presence of multiple NLRP3 positive specks throughout the neutrophils following signal 2 is clearly detected in Supplemental videos 1 and 2. To detect ASC oligomerization, neutrophils were stimulated with pneumolysin or nigericin, and lysates were cross-linked using DSS, and examined by western blot analysis using a monoclonal antibody to ASC. As shown in Figure 3F, ASC was detected as monomers in unstimulated cells, but as multimers in pneumolysin and nigericin stimulated neutrophils.

These findings demonstrate that not only do neutrophils express NLRP3 and ASC, but they also form several large multimeric complexes more typically seen in macrophages and dendritic cells.

Pneumolysin – stimulated neutrophils have multiple Caspase-1 and ASC specks

To quantify the number of Caspase-1 and ASC specks in neutrophils, bone marrow neutrophils from C57BL/6 mice were primed for 3h with hkSP followed by 2h stimulation with purified pneumolysin (Ply). Cells were then stained with antibody to ASC or with FAM-YVAD-FMK and analyzed by Amnis Imagestream, and the number of specks associated with each cell was quantified using IDEAS software. Representative neutrophils analyzed are shown as brightfield images (Channel 1, Ch01) and green fluorescent specks

(Channel 2, Ch02) expressing one or multiple ASC specks (Figure 4A, D). The majority of the neutrophils (56.2%) expressed two or more ASC specks, and the actual numbers and percentages are shown in Figure 4B, C.

Representative neutrophils stained with FAM-YVAD-FMK for caspase-1 activity are shown in Figure 4D, and quantification shows very similar numbers as ASC specks, with 66.4% neutrophils having two or more specks (Figure 4E, F). The specificity of FAM-YVAD-FMK stain was confirmed by using Caspase-1/11$^{-/-}$ neutrophils, which showed significantly reduced number of caspase-1 specks compared to C57BL/6 neutrophils after stimulation with pneumolysin (Supplemental Figure S3). The presence of caspase-1 positive cells and specks in caspase 1/11$^{-/-}$ mice is likely due to cross reactivity of FAM-YVAD-FMK with other pro-apoptotic caspases that are expressed in neutrophils.

Taken together, these data indicate that in contrast to macrophages and dendritic cells, murine bone marrow neutrophils express multiple caspase-1 and ASC specks upon activation of NLRP3 inflammasome by pneumolysin.

Caspase-1 activation in neutrophils is dependent on NLRP3 and ASC, and requires active pneumolysin

To determine whether live *S. pneumoniae* can activate caspase-1 in neutrophils, murine bone marrow neutrophils from C57BL/6 mice were incubated 3h with heat-killed *S. pneumoniae* (hkSP, Signal 1), followed by 2h stimulation with live TIGR4 *S. pneumoniae* or with an isogenic mutant deleted for the gene encoding Ply (*ply*) (Signal 2), and active caspase-1 was quantified using FLICA660-YVAD.

Caspase-1 staining was detected as speck-like structures in neutrophils following incubation with *S. pneumoniae* TIGR4 strain expressing pneumolysin, but not with the *ply* pneumolysin mutant or with hkSP alone (Figure 5A). Consistently, there was a significantly higher percent of FLICA 660 YVAD$^+$ neutrophils after incubation with live *S. pneumoniae* compared with neutrophils stimulated with the *ply* mutants or hkSP alone (Figure 5B).

To determine if recombinant pneumolysin can induce caspase-1 activation in neutrophils, bone marrow neutrophils from C57BL/6 mice were primed with heat killed *S. pneumoniae* as before, and incubated with either a highly purified pneumolysin (Ply) that has pore-forming activity, or with a mutant pneumolysin (PdB) that has a single amino acid substitution resulting in diminished hemolytic activity (14). The percent FLICA 660 YVAD$^+$ neutrophils was assessed by flow cytometry. Figure 5C shows a distinct population of FLICA660-YVAD$^+$ neutrophils following stimulation with hemolytic pneumolysin (Ply, left panel), but not with PdB (right panel). Quantification of FLICA660-YVAD$^+$ cells showed >80% caspase-1 expressing neutrophils in presence of Ply compared to <10% in PdB treated cells (Figure 5D).

To assess the role of the NLRP3 inflammasome in pneumolysin - induced caspase-1 and IL-1β processing, NLRP3$^{-/-}$, ASC$^{-/-}$ and Caspase-1/11$^{-/-}$ neutrophils were primed with hkSP and stimulated with pneumolysin as before, and the cleaved p10 form of caspase-1 in cell supernatants was TCA-precipitated and detected by western blot analysis. Caspase-1

p10 was clearly detected in supernatants from stimulated compared with unstimulated C57BL/6 neutrophils; however, caspase-1 p10 expression was markedly less in NLRP3$^{-/-}$, ASC$^{-/-}$ and Caspase-1/11$^{-/-}$ neutrophils compared with C57BL/6 neutrophils (Figure 5E). Similarly, there were significantly fewer FLICA660-YVAD^{+} cells in Caspase-1/11$^{-/-}$, NLRP3$^{-/-}$ and ASC$^{-/-}$ compared with C57BL/6 neutrophils (Figure 5F, G), and less secreted IL-1β following stimulation with live *S. pneumoniae* or purified Ply (Figure 5H).

Taken together, these data indicate that *S. pneumoniae* pore forming toxin pneumolysin induces NLRP3/ASC-dependent caspase-1 activation and IL-1β secretion by neutrophils.

Pneumolysin mediates IL-1β processing and secretion from human neutrophils

To ascertain if *S. pneumoniae* mediated activation of the NLRP3 inflammasome in human neutrophils is dependent on the hemolytic activity of pneumolysin, we stimulated human neutrophils with a Ply deletion mutant (ply) or highly purified preparations of active hemolytic pneumolysin (Ply) and the non- hemolytic (PdB) toxoid. Human peripheral blood neutrophils were primed with hkSP for 3h to induce expression of pro-IL-1β and NLRP3, and were then stimulated with live WT TIGR4 or with mutant   ply.

IL-1β production by neutrophils was increased following incubation with increasing numbers *S. pneumoniae* TIGR4; however, IL-1β was not detected when neutrophils were stimulated with the TIGR4   ply mutant (Figure 6A). Similarly, neutrophils incubated with purified pneumolysin (Ply) produced IL-1β in a dose dependent fashion, whereas the non-hemolytic pneumolysin (PdB) induced significantly less IL-1β (Figure 6B). In contrast to IL-1β, neutrophils derived CXCL8 (IL-8) production was not significantly different when neutrophils were stimulated with the *ply* mutant or the TIGR4 parent strain (Figure 6C); there was also no difference in CXCL8 in neutrophils stimulated with PdB compared with Ply (Figure 6D), indicating that the role of active pneumolysin on IL-1β release from human neutrophils is not a general phenomenon. Neutrophils incubated with either live *S. pneumoniae* or purified pneumolysin did not release lactose dehydrogenase (Figure 6E, F) indicating that IL-1β secretion by neutrophils occurs independently of pyroptosis.

These findings demonstrate that *S. pneumoniae* – induced IL-1β secretion from human neutrophils is dependent on the hemolytic activity of pneumolysin, that this role of pneumolysin is not a result of cell lysis and does not affect production of CXCL8.

Pneumolysin-induced caspase-1 activation and IL-1β secretion by neutrophils requires K^{+} efflux

As activation of NLRP3 inflammasome in macrophages and dendritic cells can occur following a loss of cytosolic K^{+} (27), we examined the effect of pneumolysin in mediating K^{+} efflux from neutrophils.

Primed human peripheral blood neutrophils were incubated for 2h with hemolytic (Ply) or non-hemolytic (PdB) pneumolysin, and total intracellular K^{+} in cell lysates was measured by atomic absorbance spectrometry. Figure 7A shows a dose dependent decrease in cell-associated K^{+} following incubation with pneumolysin, consistent with enhanced K^{+} efflux. Intracellular K^{+} was significantly lower in neutrophils incubated with PdB, thereby

indicating an essential role for pore forming activity of Ply in induction of the K^+ efflux from neutrophils. Conversely, when neutrophils were incubated in high extracellular K^+, which prevents formation of a plasma membrane K^+ gradient, the pneumolysin – induced caspase-1 activation and IL-1β secretion were completely ablated (Figure 7B, C), indicating that K^+ efflux is critical for caspase-1 activation and IL-1β secretion by pneumolysin – stimulated neutrophils.

In addition to cleaving pro-IL-1β, caspase-1 also mediates pyroptotic cell death, which is characterized by loss of plasma membrane integrity and release of cytoplasmic contents, including LDH (28, 29). We therefore examined if pneumolysin - induced K^+ efflux occurs as a secondary consequence of pyroptotic cell death, *i.e.*, after caspase-1 activation, or if K^+ efflux is an early signal for NLRP3 inflammasome assembly and IL-1β secretion, *i.e.,* before caspase-1 activation. Human neutrophils were primed with hkSP and incubated with pneumolysin or nigericin in presence of the caspase-1 inhibitor YVAD or the pan-caspase inhibitor ZVAD, and IL-1β secretion, intracellular K^+ and LDH release were measured.

As shown in Figure 7D, IL-1β secretion by neutrophils stimulated with pneumolysin or nigericin was completely inhibited in the presence of YVAD or ZVAD, indicating a requirement for caspase-1 in pneumolysin induced IL-1β secretion. In contrast, pneumolysin induced K^+ efflux (loss of intracellular K^+) was not inhibited by caspase-1 inhibitors (Figure 7E), indicating that K^+ efflux occurs upstream of caspase-1 activation. Similarly, pneumolysin – induced LDH release in the presence of caspase-1 inhibitors was not significantly different from pneumolysin alone, indicating that neutrophils are not undergoing caspase-1 dependent pyroptosis (Figure 7F).

Therefore, the results of these studies support the concept that pneumolysin induces IL-1β secretion in neutrophils by causing loss of intracellular K^+ and activation of the NLRP3 inflammasome and that K^+ efflux is an early signal for inflammasome activation in neutrophils.

Pneumolysin-induced IL-1β secretion by neutrophils does not require lysosomal disruption or serine proteases activity

Activation of the NLRP3 inflammasome in monocytes/dendritic cells can be induced by lysosomal destabilization and cathepsin B release (14, 30, 31). Additionally, since serine proteases such as neutrophil elastase can also cleave pro-IL-1β to the mature form (6, 32–34), we investigated the role of lysosomal disruption and serine proteases in Ply mediated IL-1β secretion by neutrophils.

To examine the role of cathepsin B on inflammasome activation and IL-1β release, neutrophils were incubated with purified pneumolysin or *S. pneumoniae* TIGR4 in the presence of cathepsin B inhibitors CA-074-Me, ZFA, or with bafilomycin A, which blocks lysosomal acidification by inhibiting H^+-ATPase. Figure 8A shows that IL-1β secretion by pneumolysin or *S. pneumoniae* TIGR4 –stimulated neutrophils in the presence of cathepsin B inhibitors or with bafilomycin A was not significantly different from cells in the absence of inhibitors, indicating that neither cathepsin B nor lysosomal destabilization are required for pneumolysin-induced IL-1β processing in neutrophils. LDH release was not increased

following incubation with these inhibitors, indicating that they are not cytotoxic at the concentrations used (Figure 8B).

Additionally, we found no difference in IL-1β secretion or LDH release by *S. pneumoniae*-stimulated bone marrow neutrophils from neutrophil elastase (NE)$^{-/-}$ mice compared with C57BL/6 neutrophils (Figure 8C, D), indicating that there is no role for elastase in IL-1β processing, and also that Ply - induced IL-1β processing by neutrophils does not require serine protease or cathepsin B activity.

DISCUSSION

Streptococcus pneumoniae is the causative organism of pneumococcal septicemia, meningitis, and pneumonia, which results in infant mortality on a global scale (35, 36). *S. pneumoniae* is also a leading cause of corneal ulcers worldwide resulting in visual impairment and blindness, especially in developing countries where the organisms are resident in the conjunctiva and enter the corneal stroma following an abrasion (37–39). In a study of individuals with *S. pneumoniae* corneal ulcers, neutrophils comprised over 90% of the total cells; further, expression of IL-1β, NLRP3 and ASC in corneal ulcers was greatly elevated compared with normal corneas (23).

Neutrophils are a source of pro-inflammatory and regulator cytokines, including IFN-γ and IL-17A (19, 40, 41). Further, although neutrophils are generally considered to be short-lived cells in the circulation, other reports indicate that these cells can survive for longer periods of time under inflammatory conditions where they are stimulated by pro-inflammatory cytokines and growth factors (42).

NLRP3 inflammasome activation and IL-1β processing have been extensively studied in monocytes, macrophages and dendritic cells (3, 24); however, although neutrophils are the most prominent cells infiltrating sites of infection and inflammation, the contribution of neutrophils to inflammasome activation and IL-1β production is less well understood.

Neutrophils are a major source of IL-1β in murine models of arthritis and osteomyelitis; however, as with our study on *P. aeruginosa* keratitis, IL-1β processing was caspase-1 independent and occurred as a result of cleavage by neutrophil proteases (5, 6, 43). In contrast, proteases and caspase-1 both contributed to IL-1β processing by LPS+ATP – stimulated human neutrophils (44). However, our current findings are in agreement with a report showing that neutrophils are a major source of IL-1β in a *Staphylococcus aureus* model of skin abscess formation; further, these investigators showed that *S. aureus* induced IL-1β secretion by bone marrow neutrophils was impaired in ASC$^{-/-}$ mice and in the presence of NLRP3 and caspase-1 inhibitors, and thereby implicating the NLRP3 inflammasome (45). In a separate study, IL-1β secretion by murine bone marrow neutrophils stimulated with nigericin was dependent on expression of NLRP3 and ASC (46). We also show that the NLRP3 inflammasome is required for IL-1β cleavage during *S. pneumoniae* corneal infection, and demonstrate that neutrophils recruited to infected corneas have active caspase-1 as detected by YVAD-FLICA.

In the current study, we have shown the results of multiple, highly reproducible experiments demonstrating that neutrophils form NLRP3/ASC/caspase 1 oligomers that are detected as multiple specks, including: a) the presence of caspase-1 (using FLICA-YVAD) specks in neutrophils isolated from infected corneas; b) the presence of multiple NLRP3 specks in bone marrow neutrophils following signal 1 and signal 2, as shown in Supplemental videos 1 and 2; c) the presence of ASC monomers in neutrophils given signal 1, and ASC multimeric complexes following signal 2; and c) quantification of ASC and caspase-1specks in isolated neutrophils given signals 1 and 2.

The presence of multiple specks in neutrophils is clearly distinct from dendritic cells and macrophages, which mostly show single speck per cell (3), although multiple specks were detected in macrophages from patients with a gain of function mutation in NLRC4 (47). The significance of multiple versus single inflammasome oligomers in neutrophils has yet to be determined; however, it is very clear that neutrophils are a major source of mature IL-1β, at least at early stages of infection, and that activation of caspase-1 through the NLRP3/ASC inflammasome is essential for processing IL-1β.

We reported that neutrophils are an important source of IL-1β in *Pseudomonas aeruginosa* corneal infection, and that cleavage is a result of serine protease activity and independent of caspase-1 and the NLRC4 inflammasome (6). In contrast to that study, we now show that although neutrophils are a major source of IL-1β in *S. pneumoniae* keratitis, caspase-1 is required for IL-1β cleavage, and is activated by the NLRP3/ASC inflammasome. The difference between these models may be due to relatively low NLRC4 expression by neutrophils compared with macrophages (46).

To characterize the mechanisms by which the NLRP3 inflammasome is activated in human neutrophils, we examined two pathways that have been proposed (48): a) the channel mode that results in loss of cytosolic K^+; and b) the cathepsin B pathway that is activated by lysosome rupture following phagocytosis. We also examined the role of pyroptosis in this process. Our data are consistent with the first pathway in which active pneumolysin causes loss of intracellular K^+. Because caspase-1 inhibitors blocked IL-1β secretion, but did not inhibit K^+ efflux, we conclude that pneumolysin -induced K^+ efflux occurs upstream and independently of caspase-1 mediated IL-1β processing and is not a secondary consequence of caspase-1-driven pyroptosis. This finding that NLRP3 activation in neutrophil do not lead to pyroptosis is in agreement with a recent paper demonstrating that neutrophils do not undergo NLRC4 – mediated pyroptotic cell death following stimulation with *Salmonella* (49). Although the molecular basis for the absence of pyroptosis in neutrophils compared with macrophages has yet to be defined, a possible advantage is that bacteria are released from dead macrophages and can then be killed by neutrophils (50). Further, in contrast to macrophages, neutrophils undergo netotic cell death where the nucleus decondenses and chromatin is released from the cell to form neutrophil extracellular traps (NETs), which also include together antimicrobial peptides and proteases that are effective in killing microbial pathogens (51, 52).

Lysosomal destabilization and cathepsin B activation contribute to *S. pneumoniae* induced NLRP3 activation in monocytes and macrophages (31); however, we found no role for

cathepsin B in neutrophil mediated IL-1β processing, whereas our findings on the role of K^+ efflux are consistent with a recent study showing that K^+ efflux is critical for activation of the NLRP3 inflammasome in bone marrow macrophages and dendritic cells (14, 27). Although activated in response to structurally distinct agents including silica, asbestos, uric acid crystals and bacterial toxins as well as DAMPs including ATP, a common response to all NLRP3 activating stimuli is a change in plasma membrane permeability that leads to efflux of intracellular potassium. Pneumolysin has been shown to induce K^+ efflux in macrophages (35, 53), and we now show that this is also required in human neutrophils.

Pneumolysin is an important virulence factor in *S. pneumoniae* infections, and is expressed in clinical isolates from *S. pneumoniae* infections, including corneal ulcers (23, 35). Pneumolysin is a cholesterol-dependent cytolysin toxin that forms oligomers in the host cell plasma membrane (~40 monomers), resulting in formation of large (~400 A) transmembrane pores that cause rapid cell lysis (54). Although reported as a cytoplasmic protein that is released after autolysis (35), pneumolysin was more recently shown to localize in the bacterial cell wall where it is released following cleavage by extracellular proteases (55, 56). Pneumolysin activates the NLRP3 inflammasome in monocytes, macrophages and dendritic cells in pneumococcal pneumonia (14, 57), and pneumolysin expressing *S. pneumoniae* strains induce keratitis in animal models (58, 59). In the current study, we demonstrated that NLRP3 oligomerization, caspase-1 activation and IL-1β processing in human and murine neutrophils is dependent on expression of the hemolytic activity of pneumolysin, as neither the *S. pneumoniae ply* mutant nor the non-hemolytic PdB toxoid induced this response. Similarly, *S. aureus* induced IL-1β secretion by neutrophils required expression of the pore forming alpha toxin (45).

Oligomerization of the NLRP3/ASC inflammasome can be visualized as discrete intracellular specks in macrophages and dendritic cells (3); however, we demonstrate that caspase-1 specks are generated in activated neutrophils *in vitro* and *in vivo* following *S. pneumoniae* corneal infection. We also show that ASC form multimeric complexes in pneumolysin - activated neutrophils, which is similar to that described in formation in macrophages (3, 27). However, in contrast to macrophages that have single specks (3), we consistently found that stimulated murine and human neutrophils have multiple specks. The basis for this difference has yet to be determined.

We used caspase-1$^{-/-}$ mice that are also deficient in caspase 11 activity; however, we show specific caspase-1 activity by neutrophils using FLICA-YVAD, and we block IL-1β production by neutrophils using the specific caspase-1 inhibitor YVAD. Taken together, these findings support a role for caspase-1 rather than caspase 11 in this process.

The results of the current study add substantially to our understanding of the role of neutrophil derived IL-1β in bacterial infections by demonstrating that neutrophils are not only an important source of this cytokine during bacterial infection, but also form NLRP3/ASC inflammasome aggregates *in vivo* that activate caspase-1 and mediate IL-1β cleavage and secretion. Further, although we show that requirement for K^+ efflux in pneumolysin – induced NLRP3 activation in neutrophils is similar to macrophages (14, 57), there are distinct differences between these cell types, including susceptibility to pyroptosis.

In conclusion, given the diverse infectious and inflammatory conditions where neutrophils infiltrate the tissues in large numbers, it seems highly likely that their role in IL-1β mediated inflammation will be found in multiple diseases.

Supplementary Material

Refer to Web version on PubMed Central for supplementary material.

Acknowledgments

References

1. Dinarello CA. Immunological and inflammatory functions of the interleukin-1 family. Annu Rev Immunol. 2009; 27:519–550. [PubMed: 19302047]

2. Dinarello CA, Simon A, van der Meer JW. Treating inflammation by blocking interleukin-1 in a broad spectrum of diseases. Nature reviews. Drug discovery. 2012; 11:633–652.

3. Latz E, Xiao TS, Stutz A. Activation and regulation of the inflammasomes. Nat Rev Immunol. 2013; 13:397–411. [PubMed: 23702978]

4. Gross O, Thomas CJ, Guarda G, Tschopp J. The inflammasome: an integrated view. Immunological reviews. 2011; 243:136–151. [PubMed: 21884173]

5. Guma M, Ronacher L, Liu-Bryan R, Takai S, Karin M, Corr M. Caspase 1-independent activation of interleukin-1beta in neutrophil-predominant inflammation. Arthritis Rheum. 2009; 60:3642–3650. [PubMed: 19950258]

6. Karmakar M, Sun Y, Hise AG, Rietsch A, Pearlman E. Cutting Edge: IL-1beta Processing during Pseudomonas aeruginosa Infection Is Mediated by Neutrophil Serine Proteases and Is Independent of NLRC4 and Caspase-1. J Immunol. 2012; 189:4231–4235. [PubMed: 23024281]

7. Joosten LA, Netea MG, Fantuzzi G, Koenders MI, Helsen MM, Sparrer H, Pham CT, van der Meer JW, Dinarello CA, van den Berg WB. Inflammatory arthritis in caspase 1 gene-deficient mice: contribution of proteinase 3 to caspase 1-independent production of bioactive interleukin-1beta. Arthritis and rheumatism. 2009; 60:3651–3662. [PubMed: 19950280]

8. Lamkanfi M, Dixit VM. Mechanisms and functions of inflammasomes. Cell. 2014; 157:1013–1022. [PubMed: 24855941]

9. Kuida K, Lippke JA, Ku G, Harding MW, Livingston DJ, Su MS, Flavell RA. Altered cytokine export and apoptosis in mice deficient in interleukin-1 beta converting enzyme. Science. 1995; 267:2000–2003. [PubMed: 7535475]

10. Broz P, Ruby T, Belhocine K, Bouley DM, Kayagaki N, Dixit VM, Monack DM. Caspase-11 increases susceptibility to Salmonella infection in the absence of caspase-1. Nature. 2012; 490:288–291. [PubMed: 22895188]

11. Kanneganti TD, Ozoren N, Body-Malapel M, Amer A, Park JH, Franchi L, Whitfield J, Barchet W, Colonna M, Vandenabeele P, Bertin J, Coyle A, Grant EP, Akira S, Nunez G. Bacterial RNA and small antiviral compounds activate caspase-1 through cryopyrin/Nalp3. Nature. 2006; 440:233–236. [PubMed: 16407888]

12. Sun Y, Karmakar M, Roy S, Ramadan RT, Williams SR, Howell S, Shive CL, Han Y, Stopford CM, Rietsch A, Pearlman E. TLR4 and TLR5 on corneal macrophages regulate Pseudomonas aeruginosa keratitis by signaling through MyD88-dependent and -independent pathways. J Immunol. 2010; 185:4272–4283. [PubMed: 20826748]

13. Gilbert RJ, Rossjohn J, Parker MW, Tweten RK, Morgan PJ, Mitchell TJ, Errington N, Rowe AJ, Andrew PW, Byron O. Self-interaction of pneumolysin, the pore-forming protein toxin of Streptococcus pneumoniae. J Mol Biol. 1998; 284:1223–1237. [PubMed: 9837740]

14. McNeela EA, Burke A, Neill DR, Baxter C, Fernandes VE, Ferreira D, Smeaton S, El-Rachkidy R, McLoughlin RM, Mori A, Moran B, Fitzgerald KA, Tschopp J, Petrilli V, Andrew PW, Kadioglu A, Lavelle EC. Pneumolysin activates the NLRP3 inflammasome and promotes proinflammatory cytokines independently of TLR4. PLoS pathogens. 2010; 6:e1001191. [PubMed: 21085613]

15. Franzen CA, Simms PE, Van Huis AF, Foreman KE, Kuo PC, Gupta GN. Characterization of uptake and internalization of exosomes by bladder cancer cells. BioMed research international. 2014; 2014:619829. [PubMed: 24575409]

16. Kahlenberg JM, Dubyak GR. Mechanisms of caspase-1 activation by P2X7 receptor-mediated K+ release. American journal of physiology. Cell physiology. 2004; 286:C1100–1108. [PubMed: 15075209]

17. Hamrah P, Liu Y, Zhang Q, Dana MR. The corneal stroma is endowed with a significant number of resident dendritic cells. Invest Ophthalmol Vis Sci. 2003; 44:581–589. [PubMed: 12556386]

18. Knickelbein JE, Watkins SC, McMenamin PG, Hendricks RL. Stratification of Antigen-presenting Cells within the Normal Cornea. Ophthalmol Eye Dis. 2009; 1:45–54. [PubMed: 20431695]

19. Taylor PR, Roy S, Leal SM Jr, Sun Y, Howell SJ, Cobb BA, Li X, Pearlman E. Activation of neutrophils by autocrine IL-17A-IL-17RC interactions during fungal infection is regulated by IL-6, IL-23, RORgammat and dectin-2. Nat Immunol. 2014; 15:143–151. [PubMed: 24362892]

20. Meissner F, Seger RA, Moshous D, Fischer A, Reichenbach J, Zychlinsky A. Inflammasome activation in NADPH oxidase defective mononuclear phagocytes from patients with chronic granulomatous disease. Blood. 2010; 116:1570–1573. [PubMed: 20495074]

21. Sokolovska A, Becker CE, Ip WK, Rathinam VA, Brudner M, Paquette N, Tanne A, Vanaja SK, Moore KJ, Fitzgerald KA, Lacy-Hulbert A, Stuart LM. Activation of caspase-1 by the NLRP3 inflammasome regulates the NADPH oxidase NOX2 to control phagosome function. Nature immunology. 2013; 14:543–553. [PubMed: 23644505]

22. Tullos NA, Thompson HW, Taylor SD, Sanders M, Norcross EW, Tolo I, Moore Q, Marquart ME. Modulation of immune signaling, bacterial clearance, and corneal integrity by toll-like receptors during streptococcus pneumoniae keratitis. Current eye research. 2013; 38:1036–1048. [PubMed: 23841825]

23. Karthikeyan RS, Priya JL, Leal SM Jr, Toska J, Rietsch A, Prajna V, Pearlman E, Lalitha P. Host response and bacterial virulence factor expression in Pseudomonas aeruginosa and Streptococcus pneumoniae corneal ulcers. PLoS One. 2013; 8:e64867. [PubMed: 23750216]

24. Franchi L, Munoz-Planillo R, Nunez G. Sensing and reacting to microbes through the inflammasomes. Nat Immunol. 2012; 13:325–332. [PubMed: 22430785]

25. Ataide MA, Andrade WA, Zamboni DS, Wang D, do Souza MC, Franklin BS, Elian S, Martins FS, Pereira D, Reed G, Fitzgerald KA, Golenbock DT, Gazzinelli RT. Malaria-induced NLRP12/NLRP3-dependent caspase-1 activation mediates inflammation and hypersensitivity to bacterial superinfection. PLoS pathogens. 2014; 10:e1003885. [PubMed: 24453977]

26. Subramanian N, Natarajan K, Clatworthy MR, Wang Z, Germain RN. The adaptor MAVS promotes NLRP3 mitochondrial localization and inflammasome activation. Cell. 2013; 153:348–361. [PubMed: 23582325]

27. Munoz-Planillo R, Kuffa P, Martinez-Colon G, Smith BL, Rajendiran TM, Nunez G. K(+) efflux is the common trigger of NLRP3 inflammasome activation by bacterial toxins and particulate matter. Immunity. 2013; 38:1142–1153. [PubMed: 23809161]

28. Sagulenko V, Thygesen SJ, Sester DP, Idris A, Cridland JA, Vajjhala PR, Roberts TL, Schroder K, Vince JE, Hill JM, Silke J, Stacey KJ. AIM2 and NLRP3 inflammasomes activate both apoptotic and pyroptotic death pathways via ASC. Cell Death Differ. 2013; 20:1149–1160. [PubMed: 23645208]

29. Fernandes-Alnemri T, Wu J, Yu JW, Datta P, Miller B, Jankowski W, Rosenberg S, Zhang J, Alnemri ES. The pyroptosome: a supramolecular assembly of ASC dimers mediating inflammatory cell death via caspase-1 activation. Cell Death Differ. 2007; 14:1590–1604. [PubMed: 17599095]

30. Hornung V, Bauernfeind F, Halle A, Samstad EO, Kono H, Rock KL, Fitzgerald KA, Latz E. Silica crystals and aluminum salts activate the NALP3 inflammasome through phagosomal destabilization. Nat Immunol. 2008; 9:847–856. [PubMed: 18604214]

31. Hoegen T, Tremel N, Klein M, Angele B, Wagner H, Kirschning C, Pfister HW, Fontana A, Hammerschmidt S, Koedel U. The NLRP3 inflammasome contributes to brain injury in pneumococcal meningitis and is activated through ATP-dependent lysosomal cathepsin B release. Journal of immunology. 2011; 187:5440–5451.

32. Stehlik C. Multiple interleukin-1beta-converting enzymes contribute to inflammatory arthritis. Arthritis Rheum. 2009; 60:3524–3530. [PubMed: 19950297]

33. Black RA, Kronheim SR, Cantrell M, Deeley MC, March CJ, Prickett KS, Wignall J, Conlon PJ, Cosman D, Hopp TP, et al. Generation of biologically active interleukin-1 beta by proteolytic cleavage of the inactive precursor. J Biol Chem. 1988; 263:9437–9442. [PubMed: 3288634]

34. Hazuda DJ, Strickler J, Kueppers F, Simon PL, Young PR. Processing of precursor interleukin 1 beta and inflammatory disease. J Biol Chem. 1990; 265:6318–6322. [PubMed: 2156847]

35. Kadioglu A, Weiser JN, Paton JC, Andrew PW. The role of Streptococcus pneumoniae virulence factors in host respiratory colonization and disease. Nat Rev Microbiol. 2008; 6:288–301. [PubMed: 18340341]

36. Denny FW, Loda FA. Acute respiratory infections are the leading cause of death in children in developing countries. Am J Trop Med Hyg. 1986; 35:1–2. [PubMed: 3946732]

37. Bharathi MJ, Ramakrishnan R, Meenakshi R, Padmavathy S, Shivakumar C, Srinivasan M. Microbial keratitis in South India: influence of risk factors, climate, and geographical variation. Ophthalmic Epidemiol. 2007; 14:61–69. [PubMed: 17464852]

38. Parmar P, Salman A, Kalavathy CM, Jesudasan CA, Thomas PA. Pneumococcal keratitis: a clinical profile. Clin Experiment Ophthalmol. 2003; 31:44–47. [PubMed: 12580893]

39. Upadhyay MP, Karmacharya PC, Koirala S, Tuladhar NR, Bryan LE, Smolin G, Whitcher JP. Epidemiologic characteristics, predisposing factors, and etiologic diagnosis of corneal ulceration in Nepal. Am J Ophthalmol. 1991; 111:92–99. [PubMed: 1985498]

40. Mantovani A, Cassatella MA, Costantini C, Jaillon S. Neutrophils in the activation and regulation of innate and adaptive immunity. Nat Rev Immunol. 2011; 11:519–531. [PubMed: 21785456]

41. Sturge CR, Benson A, Raetz M, Wilhelm CL, Mirpuri J, Vitetta ES, Yarovinsky F. TLR-independent neutrophil-derived IFN-gamma is important for host resistance to intracellular pathogens. Proc Natl Acad Sci U S A. 2013; 110:10711–10716. [PubMed: 23754402]

42. Kolaczkowska E, Kubes P. Neutrophil recruitment and function in health and inflammation. Nat Rev Immunol. 2013; 13:159–175. [PubMed: 23435331]

43. Cassel SL, Janczy JR, Bing X, Wilson SP, Olivier AK, Otero JE, Iwakura Y, Shayakhmetov DM, Bassuk AG, Abu-Amer Y, Brogden KA, Burns TL, Sutterwala FS, Ferguson PJ. Inflammasome-independent IL-1beta mediates autoinflammatory disease in Pstpip2-deficient mice. Proceedings of the National Academy of Sciences of the United States of America. 2014; 111:1072–1077. [PubMed: 24395802]

44. Gabelloni ML, Sabbione F, Jancic C, Bass JF, Keitelman I, Iula L, Oleastro M, Geffner JR, Trevani AS. NADPH oxidase derived reactive oxygen species are involved in human neutrophil IL-1beta secretion but not in inflammasome activation. European journal of immunology. 2013

45. Cho JS, Guo Y, Ramos RI, Hebroni F, Plaisier SB, Xuan C, Granick JL, Matsushima H, Takashima A, Iwakura Y, Cheung AL, Cheng G, Lee DJ, Simon SI, Miller LS. Neutrophil-derived IL-1beta is sufficient for abscess formation in immunity against Staphylococcus aureus in mice. PLoS pathogens. 2012; 8:e1003047. [PubMed: 23209417]

46. Mankan AK, Dau T, Jenne D, Hornung V. The NLRP3/ASC/Caspase-1 axis regulates IL-1beta processing in neutrophils. European journal of immunology. 2012; 42:710–715. [PubMed: 22213227]

47. Romberg N, Al Moussawi K, Nelson-Williams C, Stiegler AL, Loring E, Choi M, Overton J, Meffre E, Khokha MK, Huttner AJ, West B, Podoltsev NA, Boggon TJ, Kazmierczak BI, Lifton RP. Mutation of NLRC4 causes a syndrome of enterocolitis and autoinflammation. Nature genetics. 2014; 46:1135–1139. [PubMed: 25217960]

48. Tschopp J, Schroder K. NLRP3 inflammasome activation: The convergence of multiple signalling pathways on ROS production? Nat Rev Immunol. 2010; 10:210–215. [PubMed: 20168318]

49. Chen KW, Gross CJ, Sotomayor FV, Stacey KJ, Tschopp J, Sweet MJ, Schroder K. The Neutrophil NLRC4 Inflammasome Selectively Promotes IL-1beta Maturation without Pyroptosis during Acute Salmonella Challenge. Cell reports. 2014; 8:570–582. [PubMed: 25043180]

50. Miao EA, Leaf IA, Treuting PM, Mao DP, Dors M, Sarkar A, Warren SE, Wewers MD, Aderem A. Caspase-1-induced pyroptosis is an innate immune effector mechanism against intracellular bacteria. Nature immunology. 2010; 11:1136–1142. [PubMed: 21057511]

51. Brinkmann V, Reichard U, Goosmann C, Fauler B, Uhlemann Y, Weiss DS, Weinrauch Y, Zychlinsky A. Neutrophil extracellular traps kill bacteria. Science. 2004; 303:1532–1535. [PubMed: 15001782]

52. Kaplan MJ, Radic M. Neutrophil extracellular traps: double-edged swords of innate immunity. Journal of immunology. 2012; 189:2689–2695.

53. Franchi L, Kanneganti TD, Dubyak GR, Nunez G. Differential requirement of P2X7 receptor and intracellular K+ for caspase-1 activation induced by intracellular and extracellular bacteria. J Biol Chem. 2007; 282:18810–18818. [PubMed: 17491021]

54. Tilley SJ, Orlova EV, Gilbert RJ, Andrew PW, Saibil HR. Structural basis of pore formation by the bacterial toxin pneumolysin. Cell. 2005; 121:247–256. [PubMed: 15851031]

55. Price KE, Camilli A. Pneumolysin localizes to the cell wall of Streptococcus pneumoniae. J Bacteriol. 2009; 191:2163–2168. [PubMed: 19168620]

56. Price KE, Greene NG, Camilli A. Export requirements of pneumolysin in Streptococcus pneumoniae. Journal of bacteriology. 2012; 194:3651–3660. [PubMed: 22563048]

57. Witzenrath M, Pache F, Lorenz D, Koppe U, Gutbier B, Tabeling C, Reppe K, Meixenberger K, Dorhoi A, Ma J, Holmes A, Trendelenburg G, Heimesaat MM, Bereswill S, van der Linden M, Tschopp J, Mitchell TJ, Suttorp N, Opitz B. The NLRP3 inflammasome is differentially activated by pneumolysin variants and contributes to host defense in pneumococcal pneumonia. Journal of immunology. 2011; 187:434–440.

58. Moore QC 3rd, McCormick CC, Norcross EW, Onwubiko C, Sanders ME, Fratkin J, McDaniel LS, O'Callaghan RJ, Marquart ME. Development of a Streptococcus pneumoniae keratitis model in mice. Ophthalmic Res. 2009; 42:141–146. [PubMed: 19628954]

59. Reed JM, O'Callaghan RJ, Girgis DO, McCormick CC, Caballero AR, Marquart ME. Ocular virulence of capsule-deficient streptococcus pneumoniae in a rabbit keratitis model. Invest Ophthalmol Vis Sci. 2005; 46:604–608. [PubMed: 15671288]
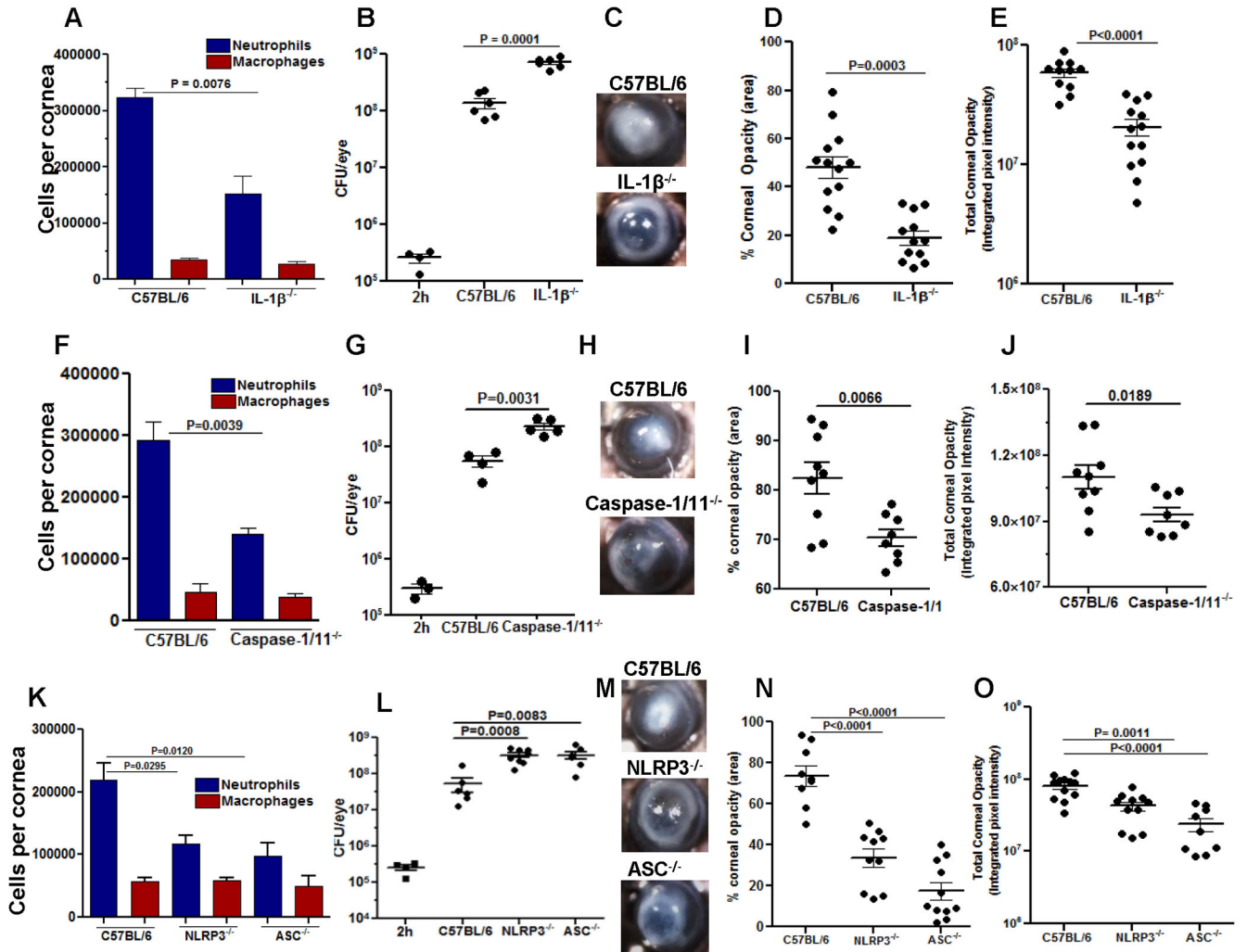
Figure 1. The role of IL-1β NLRP3, ASC and Caspase-1 in *S. pneumoniae* keratitis
C57BL/6, IL-1β$^{-/-}$, Caspase-1/11$^{-/-}$ NLRP3$^{-/-}$ and ASC$^{-/-}$ mice were infected in the corneal stroma with *S. pneumoniae* TIGR4. **A, F, K**: Total NIMP-R14$^+$ neutrophils and F4/80$^+$ macrophages in infected corneas were quantified by flow cytometry. **B, G, L**: Total CFU in eyes of infected mice after 2 h (inoculum) and after 24 h. **C, H, M**: Representative bright field images of corneas 24h post-infection; **D, I, N**: Percent, and **E, J, O** total corneal opacification calculated by Metamorph analysis as shown in Supplemental Figure S1. **A, F, K:** mean ±SD of 5 samples per group. For CFU and corneal opacification graphs, each data point represents a single cornea. Results are representative of three independent experiments with at least five mice per group.
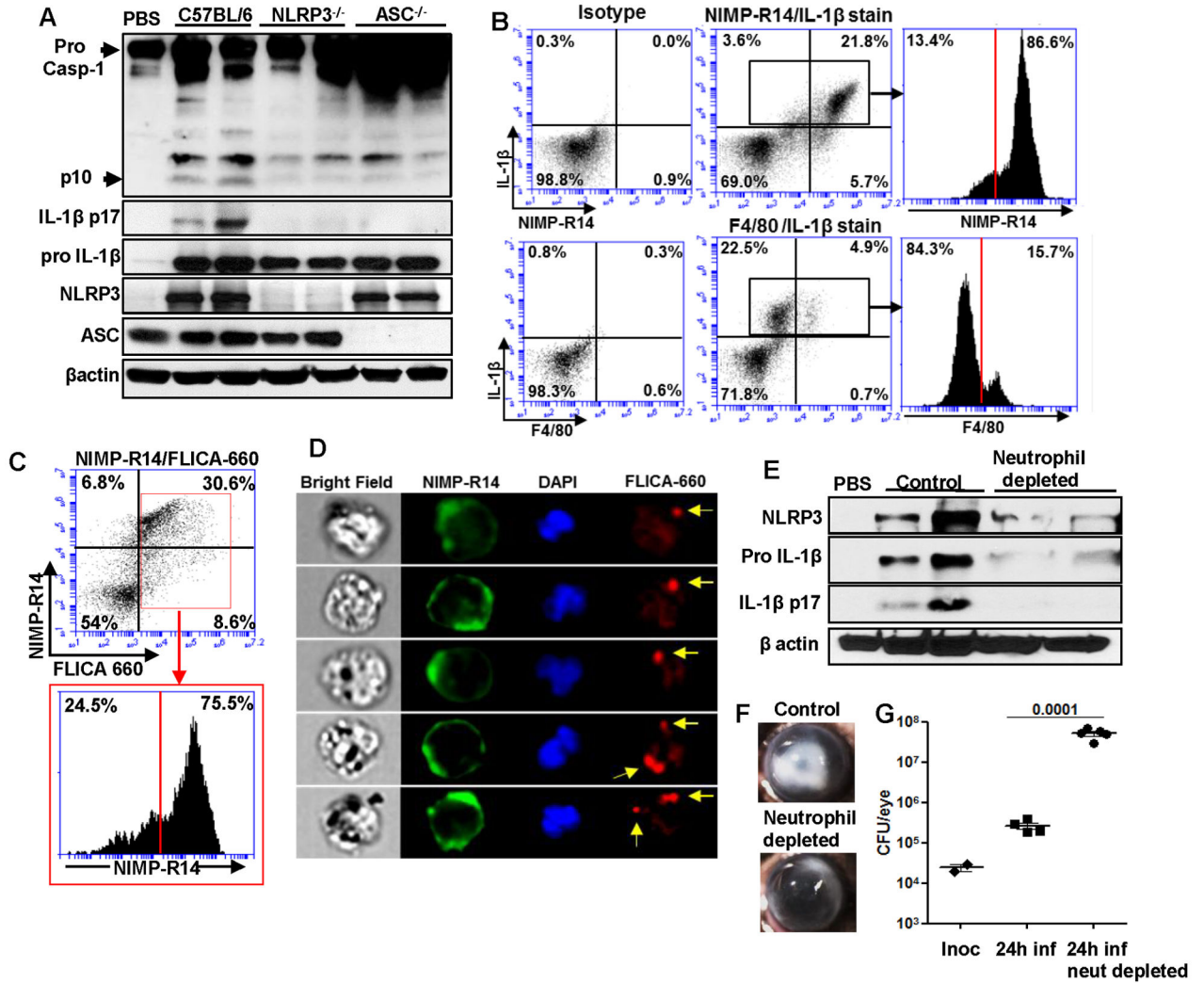
Figure 2. NLRP3 and ASC are required for caspase-1 activation and IL-1β processing by neutrophils during S. pneumoniae corneal infection

C57BL/6, NLRP3$^{-/-}$ and ASC$^{-/-}$ mice were infected in the corneal stroma with *S. pneumoniae* TIGR4 **A.** 24h post infection, corneas were excised and homogenized in lysis buffer and western blot was performed for mature forms of Caspase 1 (p10) and IL-1β (p17) are indicated by arrow heads. **B.** Flow cytometric analysis of intracellular pro IL-1β in NIMP-R14$^+$ and F4/80$^+$ cells from infected C57BL/6 corneas after 24h. Gates were determined based on an isotype control. **C–E**. C57BL/6 mice were infected with *S. pneumoniae* and 24h later corneas were excised and digested in collagenase. Total corneal cells were incubated with NIMP-R14 and FLICA-660-YVAD to detect active caspase-1 producing neutrophils by flow cytometry (**C**). NIMP-R14 (green) and FLICA-660-YVAD (red) cells were detected by multi spectral imaging flow cytometry (MIFC) (**D**), original magnification is x60. **EG**. Neutrophils were depleted in C57BL/6 mice by i.p injection of NIMP-R14 antibody 24h prior to infection with *S. pneumoniae* TIGR4. 24h post infection, corneas were excised and homogenized in lysis buffer, and western blot was performed for NLRP3, pro- and mature IL-1β (**E**). Representative brightfield images show corneal
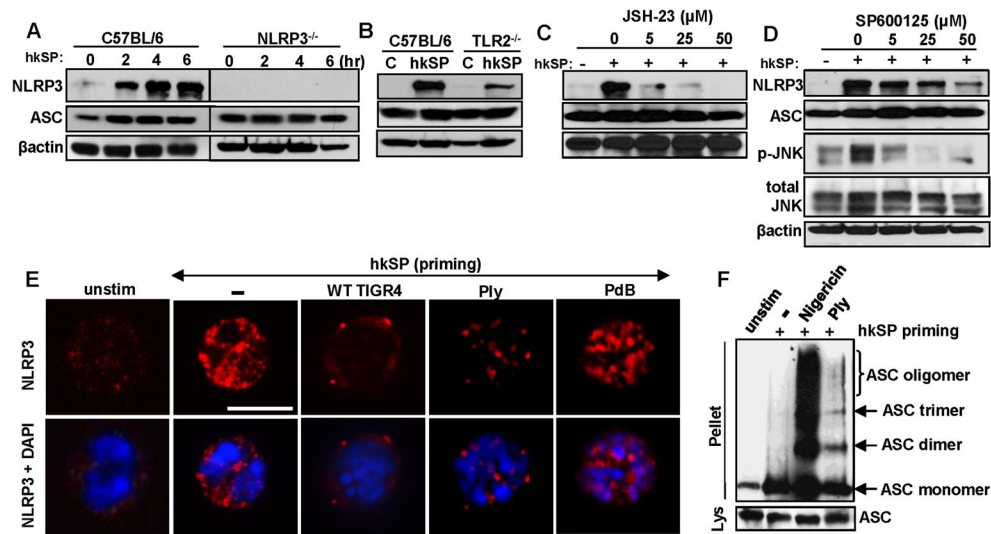
opacification (**F**), (original magnification is x20). **G.** CFU in infected eyes was quantified 24h after infection. Data points represent individual eyes. These experiments were repeated twice with similar results.
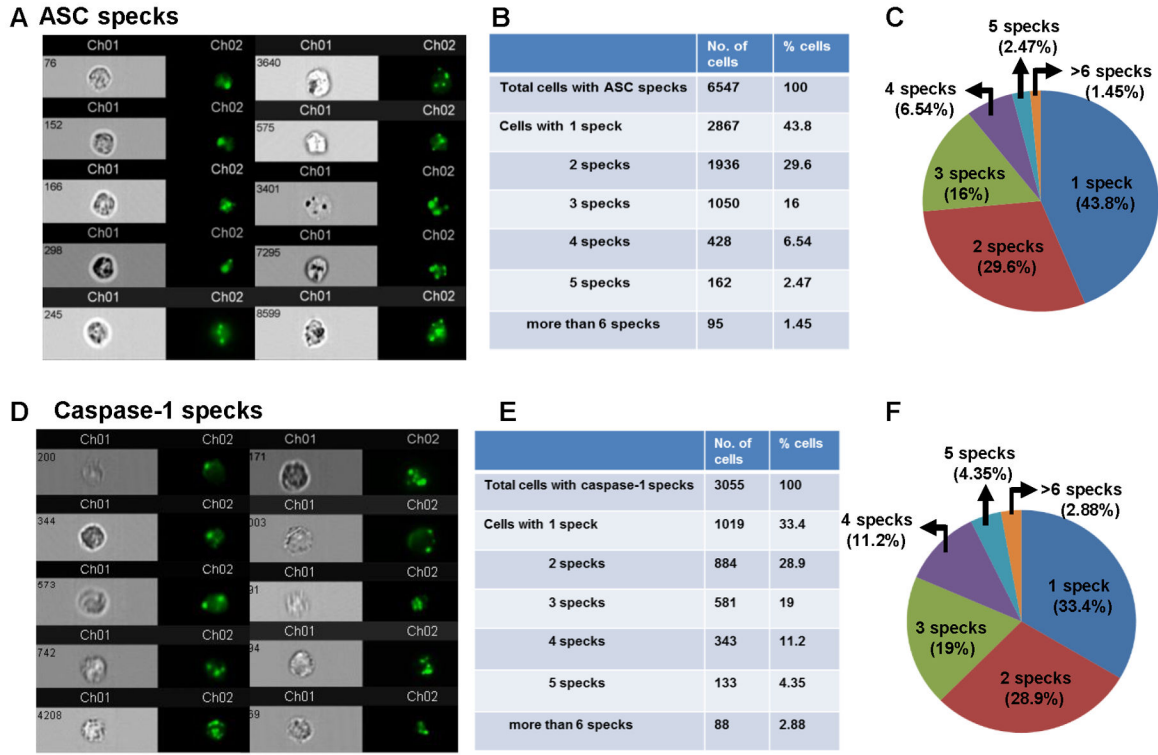
Figure 3. NLRP3/ASC expression and oligomerization in neutrophils
A. NLRP3 protein expression by western blot of C57BL/6 bone marrow neutrophils after incubation with killed *S. pneumoniae* (hkSP) for 3h. **B.** NLRP3 protein expression in bone marrow neutrophils from C57BL/6 and TLR2$^{-/-}$ mice after stimulation with hkSP for 3h **C, D.** NLRP3 expression in C57BL/6 neutrophils incubated with either NFκB inhibitor JSH-23 (**C**) or the JNK/AP-1 inhibitor SP600125 (**D**) at the indicated concentrations (μM) for 30mins prior to stimulation with hkSP for 3h. Western blot was performed for NLRP3, ASC, p-JNK, total JNK and β-actin. **E.** NLRP3 expression in C57BL/6 bone marrow neutrophils after priming with hkSP for 3h followed by stimulation with WT TIGR4 (MOI 50), Ply or a non-hemolytic Ply (PdB) for 1.5h. Red is NLRP3 and blue is DAPI; scale bar is 10μm. **F.** ASC oligomers detected by western blot from C57BL/6 bone marrow neutrophils after priming with hkSP for 3h followed by stimulation with Ply (500ng/ml) for 2h or with Nigericin (10μM) for 45mins. Western blot was performed from the pellet and lysate (Lys) using anti-ASC antibody. Data are representative of two repeat experiments.

A ASC specks

B

	No. of cells	% cells
Total cells with ASC specks	6547	100
Cells with 1 speck	2867	43.8
2 specks	1936	29.6
3 specks	1050	16
4 specks	428	6.54
5 specks	162	2.47
more than 6 specks	95	1.45

C

D Caspase-1 specks

E

|	No. of cells	% cells
Total cells with caspase-1 specks	3055	100
Cells with 1 speck	1019	33.4
2 specks	884	28.9
3 specks	581	19
4 specks	343	11.2
5 specks	133	4.35
more than 6 specks	88	2.88

F

**Figure 4. Multiple Caspase-1 and ASC specks in neutrophils**

Bone marrow neutrophils were isolated from C57BL/6 mice and primed for 2hr with hkSP and stimulated with purified Ply for 2hr. Cells were then stained with antibody to ASC or with FAM-YVAD-FMK (for caspase-1). **A.** Representative bright field and fluorescent images (60x) of neutrophils showing ASC specks. **B, C**. 6547 neutrophils were analyzed by Amnis Imagestream X and spot counting was performed using IDEAS software, and Tables and pie charts were generated showing percentage and total number of neutrophils with one or multiple ASC specks. **D.** Representative bright field and fluorescent images (60x) of neutrophils showing caspase-1 speck (FAM-YVAD-FMK staining). **E, F.** Percentage and total number of neutrophils with one or multiple caspase-1specks (3055 cells were analyzed).
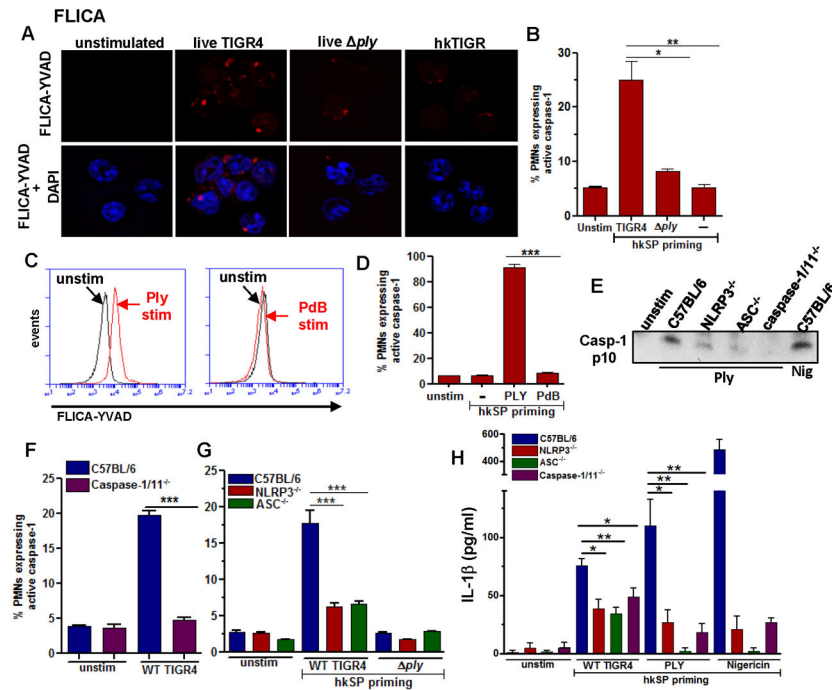
Figure 5. Active caspase-1 induction in murine neutrophils is dependent on NLRP3 and ASC, and requires active pneumolysin

C57BL/6 neutrophils were incubated 3h with heat killed *S. pneumoniae* (hkSP) (Signal 1), followed by 1.5 h stimulation with either live *S. pneumoniae* TIGR4 (WT), or the *ply* mutant (Signal 2), and active caspase-1 was detected using FLICA 660-YVAD. **A.** Representative neutrophils showing FLICA660-YVAD positive cells (red specks) (original magnification is x100). **B.** Percent FLICA660-YVAD positive neutrophils. **C, D.** Representative flow cytometry profiles (**C**) and percent (**D**) FLICA660-YVAD positive C57BL/6 neutrophils primed with hkSP and further incubated with Ply or the non-hemolytic Ply (PdB) for 1.5h. **E.** Mature p10 form of caspase-1 from supernatant of C57BL/6, NLRP3$^{-/-}$, ASC$^{-/-}$ and Caspase-1/11$^{-/-}$ neutrophils after incubation with Ply (500ng/ml) for 2h or with nigericin as a positive control. **F, G.** Percent FLICA660-YVAD positive neutrophils from C57BL/6 and caspase-1/11$^{-/-}$ mice (**F**) and from NLRP3$^{-/-}$ and ASC$^{-/-}$ mice (**G**) following hkSP priming for 3h and stimulation with live WT or *ply* mutants for 1.5h. **H**. IL-1β secretion after hkSP priming and stimulation with WT TIGR4, purified Ply (500 ng/ml) for 2h or nigericin for 45mins. Data are representative of three repeat experiments.
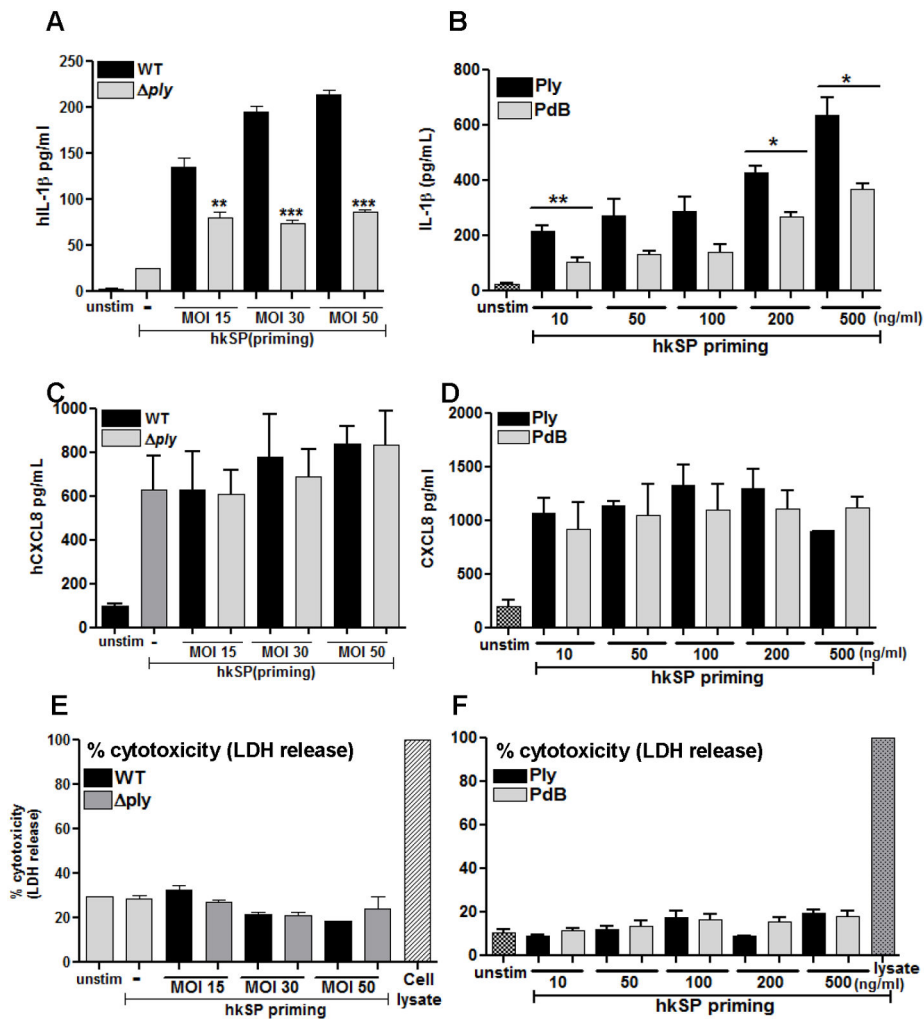
Figure 6. Pneumolysin dependent caspase-1 activation and IL-1β secretion by human neutrophils
Human peripheral blood neutrophils were primed with hkSP for 3h followed by 2h
stimulation with WT or   ply (**A, C, E**) or with Ply and PdB for 2h (**B, D, F**) and IL-1β (**A,
B**) and CXCL-8 (**C, D**) in the supernatant was quantified by ELISA. Cell death was assayed
by LDH release compared with lysed cells (**E, F**). Histograms are mean ±SD of atleast 5
samples per group and data shown are representative of three independent experiments. **
p< 0.001, *** p< 0.0001. Nig: Nigericin incubation was for 45mins.
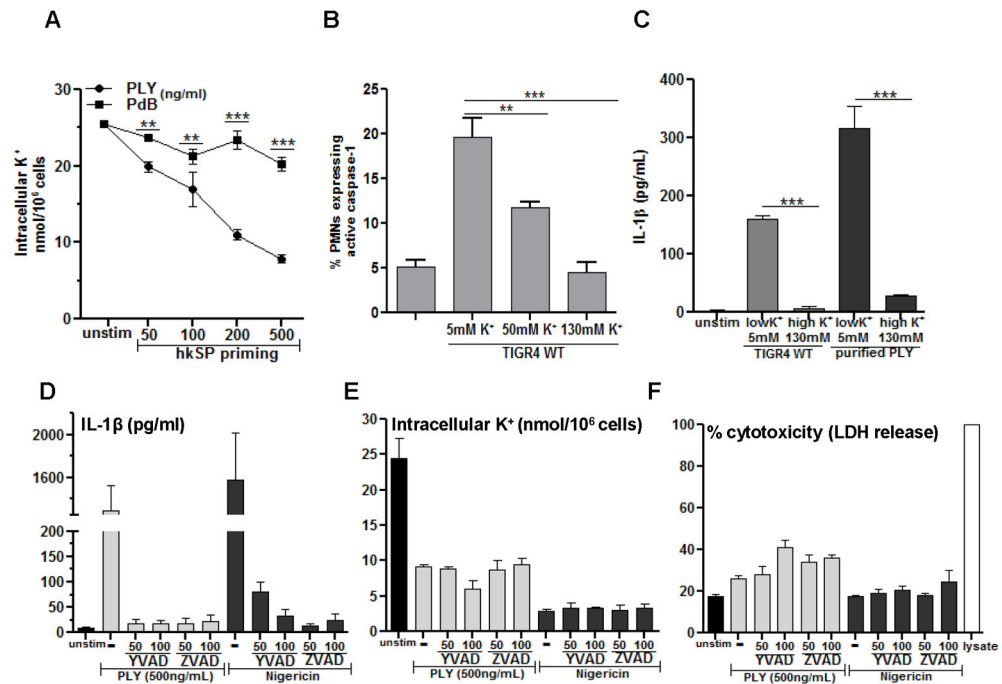
Figure 7. Pneumolysin-induced caspase-1 activation and IL-1β secretion by neutrophils requires K$^+$ efflux

A. Human peripheral blood neutrophils were hkSP primed with hkSP for 3h and stimulated with Ply or PdB for 2h. Total cell contents were extracted using 10% HNO3, and the cell associated K$^+$ concentration was quantified by atomic absorbance spectroscopy. **B.** FLICA660-YVAD positive murine neutrophils quantified by flow cytometry after treatment with live TIGR4 in presence of increasing concentration of extracellular KCl.; **C.** hkSP primed neutrophils were stimulated 2h with either Ply (500ng/ml) or WT TIGR4 (50:1) in the presence of 5 mM or 130 mM KCl, and IL-1β secretion was measured. **D–F**. Neutrophils were primed and stimulated with Ply (500ng/ml), or were stimulated with Nigericin in the presence of the pan-caspase inhibitor ZVAD or the caspase-1 inhibitor YVAD at the indicated concentration (μM), and examined for IL-1β secretion after 2hr (**D**), intracellular K$^+$ (**E**) and LDH (**F**). Histograms are mean ±SD of three samples per treatment condition, and are representative of two similar experiments with neutrophils from different donors. ** p< 0.001, *** p< 0.0001.
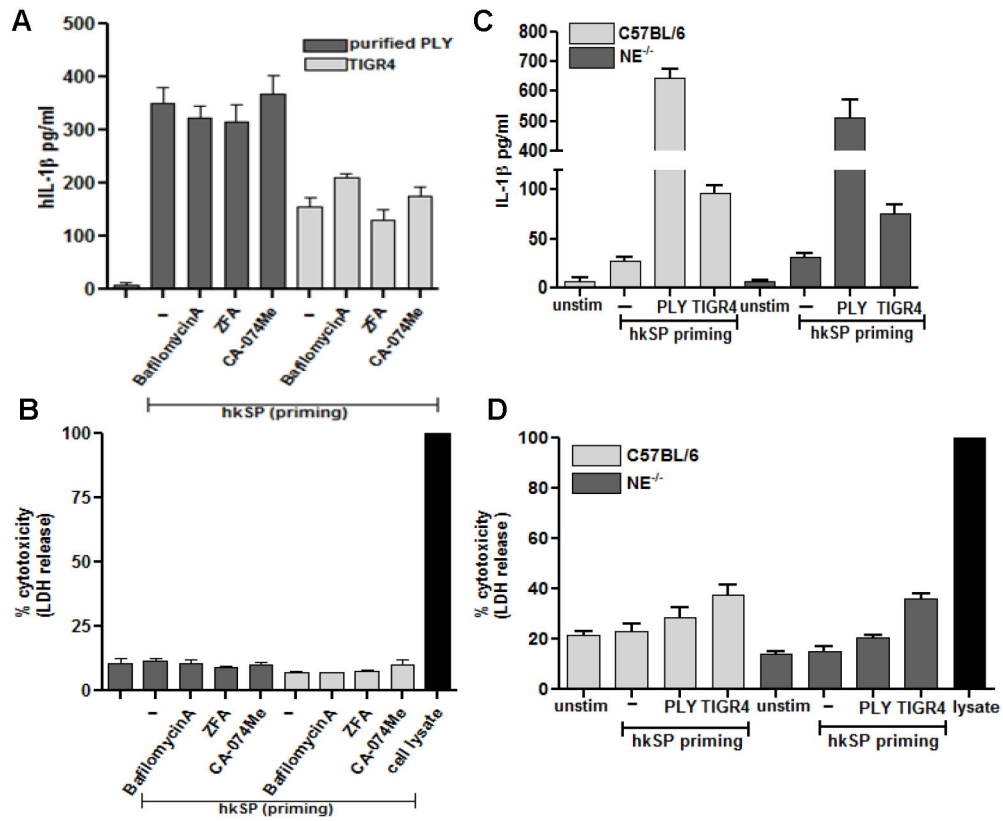
Figure 8. Pneumolysin induced IL-1β secretion by neutrophils does not require lysosomal disruption or serine protease activity

A, B. Primed human neutrophils were pretreated with bafilomycinA (200nM), CA-074-Me (100μM) or ZFA (50 μM) 30mins prior to stimulation with TIGR4 (50:1) or Ply (500ng/ml) for 2h and IL-1β **(A)** and LDH **(B)** release were quantified from the supernatant. **C, D**. Primed murine neutrophils from C57BL/6 and neutrophil elastase (NE)$^{-/-}$ were stimulated with TIGR4 (50:1) or Ply (500ng/ml) for 2h and IL-1β **(C)** and LDH **(D)** release were quantified. Histograms are mean ±SD of samples of 5 samples per treatment conditions, and are representative of three independent experiments with similar observations.